Dalton Transactions

Accepted Manuscript

ROYAL SOCIETY OF CHEMISTRY

www.rsc.org/dalton

Dalton Transactions

RSCPublishing

ARTICLE

New layered copper 1,3,5-benzenetriphosphonates pillared with N-donor ligands: Synthesis, crystal structures, and adsorption properties

Cite this: DOI: 10.1039/xoxxoooooox

Received ooth January 2012,
Accepted ooth January 2012

DOI: 10.1039/xoxxoooooox

www.rsc.org/

Atsushi Kondo, Tokuya Satomi, Kanami Azuma, Rie Takeda, Kazuyuki Maeda*,

Synthesis, crystal structures, and adsorption properties of a series of pillared layered copper phosphonates are reported. Hydrothermal reaction of copper oxide, 1,3,5-benzenetriphosphonic acid (BTP = H_6bpt), and N-donor ligands with different lengths gives three new and one reported copper organophosphonates. X-ray crystal structural analyses revealed that compound **1**, [$Cu_2(H_4btp)_2(pyr)$] (pyr = pyrazine), forms a dense 3D network structure without open pores, and on other hand compounds **2**-**4**, [$Cu_2(H_2btp)(H_2O)_2(L)$] (L = bipyridine for **2**, 1,2-bis(4-pyridyl)ethylene for **3**, and 1,3-bis(4-pyridyl)propane for **4**), show topologically identical pillared layered frameworks with micropores. The framework structures are composed of copper phosphonate layers and N-donor ligands expanding the interlayer distances. Guest water molecules occupy the pores and are removable by drying treatment. Compounds **2**-**4** adsorb and desorb water molecules reversibly with structural transformation. Interestingly, compound **3** adsorbs CO_2 and ethanol molecules in spite of no adsorption of N_2 molecules, indicating selective adsorption properties based not on molecular size but on the molecular affinities to the surfaces.

Introduction

Recently, metal-organic frameworks (MOFs), which are composed of metal ions or metal clusters and organic ligands, have emerged as a new porous materials with structural diversities and designability.[1–10] Especially, MOFs provide finely controlled structures by selecting and combining building units, and therefore the functionalities of the MOFs have been explored in academic and practical points of view. Metal organophosphonates are important class of MOF-related materials and have received much attention because of their potential applications in such areas as molecular adsorption/separation,[11–15] catalysis,[16–19] ion exchange,[20–22] magnetism,[23–28] and proton conductivity.[29–33] They often exhibit relatively high thermal and chemical stability because of stable P-C bonds and perhaps the presence of stable metal phosphonate clusters or networks in their frameworks. They also show various connection networks with different number of P-O-M bonds between metals and phosphonate groups, resulting in a variety of framework structures like chains, layers, and three dimensional open-frameworks.

Reaction of metal cations and monophosphonic acids generally tends to form layered materials covered with inert organic groups, resulting in stable layered materials with poor reactivities.[34–38] Similarly, use of diphosphonic acids with metal sources often forms dense pillared layered structures, which are composed of alternating inorganic metal phosphonate layers and organic pillar moieties.[39–43] Use of tri-functional or higher functional organophosphonic acids has been explored to avoid formation of such conventional dense pillared layered structures and several groups including us successfully synthesized metal organophosphonates with unique framework structures and properties.[44–52] For example, by using tri-functional organophosphonic acid 1,3,5-benzenetriphosphonic acid (BTP = H_6btp), we synthesized a layered zinc phosphonate $Zn_2[C_6H_3(PO_3)_2PO_3H]$•$0.5H_2$bpy•$H_2O$ (ZnBP-bpy), which is composed of anionic metal phosphonate layers and protonated 4,4'-bipyridine cations, by a hydrothermal reaction.[49] Interestingly, ZnBP-bpy shows a topotactic transformation to a zeolite-like open-framework with selective cation exchange properties.[50] Shimizu *et al*. reported proton conduction via ordered water molecules in a 2D phosphonate MOF with a layer structure closely resembling that of ZnBP-bpy.[30]

However, such metal organophosphonates with multi-functional phosphonates are still limited and adsorption properties of them are rarely investigated with several kinds of gases.[15,48,52]

Here, we show synthesis, crystal structures, and gas adsorption properties of a series of copper phosphonates with N-donor ligands as pillar molecules. Four N-donor ligands of pyrazine (pyr), 4,4′-bipyridine (bpy), trans-1,2-bis(4-pyridyl)ethylene (bpe), and 1,3-bis(4-pyridyl)propane (bpp) were selected as the pillar ligands. It is well known that these pillar molecules have potential to expand interlayer distances of layered materials. Actually, the obtained copper phosphonates have interlayer spaces corresponding to the size of each pillar molecules used and the interlayer distances are in 0.9 nm – 1.8 nm based on the crystal structures. Although compound **1**, $[Cu_2(H_4btp)_2(pyr)]$, is a nonporous material because of the small molecular size of pyr, compounds **2-4**, $[Cu_2(H_2btp)(H_2O)_2(\mathbf{L})]$ (**L** = bpy for **2**, bpe for **3**, and bpp for **4**) show porous structures. Compounds **2-4** adsorb and desorb water molecules reversibly with structural transformation. Interestingly, compounds **2-4** adsorb CO_2 and ethanol vapor in spite of no adsorption of N_2 molecules, indicating selective adsorption properties based not on molecular size but on the molecular affinities to the surfaces.

Experimental

Synthesis and characterization

General Remarks

All chemicals except BTP were used as purchased without further purification. BTP was prepared from arylphosphonate ester 1,3,5-$C_6H_3[PO(OiPr)_2]_3$ (BTPP). BTPP was prepared by a Ni-catalyzed variant of the Arbusov reaction starting from 1,3,5-tribromobenzene according to the literature.[47,53] After purification by reduced-pressure distillation of the BTPP, BTP was obtained by a simple hydrolysis reaction of BTPP with 1 M hydrochloric acid as white powder.

Characterization

CHN elemental analysis was performed on a Perkin-Elmer Series II CHNS/O analyzer 2400. Fourier transform infrared (FT-IR) spectra were recorded on a JEOL JIR-WINSPEC50 over the range 4000-600 cm^{-1} by averaging 128 scans. TG-DTA was measured in the temperature range of 25 – 1000 ºC on a Rigaku Thermo Plus 2 at a heating rate of 10 K min^{-1} under an air flow at 100 – 120 ml min^{-1}. Powder X-ray diffraction (XRD) patterns except the high resolution data used for the structure solution and indexing were measured on a Rigaku RINT-2100S diffractometer using monochromated Cu-Kα radiation. Nitrogen gas adsorption isotherms were obtained by using an automatic volumetric gas adsorption instrument Bel Japan Belsorp 28 at 77 K. Adsorption isotherms of CO_2 gas at 273 K, and water and ethanol vapor at 303 K were recorded on Bel Japan Belsorp 18. As a standard pretreatment, samples were treated under high vacuum (10^{-2} – 10^{-3} Pa) at 423 K for 3 h. By optimizing the degassing condition, samples were also evacuated at room temperature. SEM observation was performed on a JEOL JSM-6510 electron microscope at an accelerating voltage of 15 kV (Figure 1). All the compounds shows block-shaped crystals except compound **2**. The size of the crystals are in several tens of micrometer to several millimeters. Meanwhile, compound **2** shows aggregation of plate-shaped crystals in smaller crystal size. Crystals of compound **4** have many cracks on the surfaces and are confirmed to have stacking plates, implying a layered structure (Supporting information, Figure 1S).

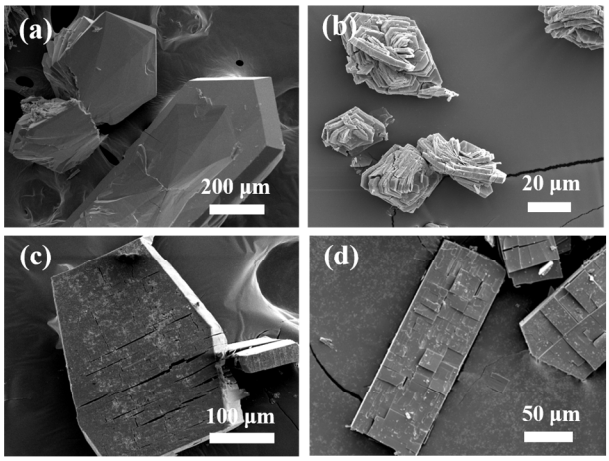

Figure 1. SEM images of compound (a) **1**, (b) **2**, (c) **3**, and (d) **4**.

Synthesis of the compounds 1-4

All the compounds **1-4** were prepared through hydrothermal reaction of aqueous mixtures of copper oxides, BTP, and N-donor ligands. Powder CuO (7.96 mg, 1.0 mmol), BTP (159 mg, 0.50 mmol), N-donor ligand (0.50 mmol), and water (2.7 ml) was put in a Teflon vessel. A typical molar ratio of CuO, BTP, N-donor ligands, and H_2O was 2 : 1 : 1 : 300. The mixture was first stirred at an ambient temperature for 1 h, and the resulting mixture was hydrothermally reacted in a 23 mL Teflon-lined stainless steel autoclave for 48 h. The material was obtained after filtration, washing by water, and drying. As N-donor ligands, pyrazine, 4,4′-bipyridine, 1,2-di(4-pyridyl)ethylene, and 1,3-di(4-pyridly)propane were used in each synthesis for compounds **1**, **2**, **3**, and **4**. The reaction temperature was 100°C for compounds **1** and **4**, and 140°C for compounds **2** and **3**. The compounds **1-4** have adsorbed water molecules on the surface and inside of the crystals and desorbed all or part of the water. Therefore, the calculated CHN values are based on the chemical compositions including/excluding guest water molecules. The compound **1**, $C_{16}H_{14}Cu_2N_2P_6O_{19}$: calcd. C 22.4, H 1.6, N 3.3 %; found C 21.5, H 1.4, N 3.1 %. IR: ν = 3125 (vw), 3071 (vw), 1417 (w), 1402 (vw), 1204 (w), 1155 (vw), 1120 (s), 1087 (m), 1065 (m), 1001(w), 945 (w), 930 (m), 913 (m), 885 (w), 806(s), 695 (s) cm^{-1}. The compound **2**, $C_{16}H_{17}Cu_2N_2P_3O_{11}$: calcd. C 30.4, H 2.7, N 4.4 %; found C

30.3, H 2.2, N 4.0 %. IR: ν = 3078 (vw), 1610 (w), 1601 (w), 1538 (vw), 1488 (w), 1409 (w), 1241 (vw), 1227 (vw), 1214 (vw), 1186 (vw), 1107 (s), 1075 (w), 1037 (s), 996 (m), 980 (m), 931 (m), 893 (m), 815 (s), 760 (w), 726 (w), 697 (m), 641 (s) cm^{-1}. The compound **3**, $C_{18}H_{27}Cu_2N_2P_3O_{15}$: calcd. C,29.6, H 3.7, N 3.8 %; found C, 28.9, H 3.4, N 3.7 %. IR: ν = 3099 (vw), 1616 (m), 1506 (vw), 1429 (vw), 1406 (w), 1251 (vw), 1210 (vw), 1117 (s), 1066 (w), 1024 (s), 995 (m), 950 (m), 915 (w), 895 (w), 838 (m), 822 (w), 698 (m) cm^{-1}. The compound **4**, $C_{18}H_{27}Cu_2N_2P_3O_{13}$: calcd. C 30.4, H 2.8, N 3.9; found C 30.3, H 2.8, N 3.7 %. IR: ν = 3013 (vw), 1618 (m), 1502 (vw), 1428 (w), 1405 (w), 1249 (vw), 1221 (vw), 1209 (vw), 1127 (m), 1186 (vw), 1127 (m), 1090 (w), 1064 (w), 1036 (s), 1023 (s), 996 (w), 953 (s), 8952(w), 821 (m), 757 (vw) cm^{-1}.

Structural analysis

Compounds **1** and **3** were obtained as large single crystals suitable for X-ray single crystal analysis and evaluated according to the procedure of single crystal structural analysis. Suitable single crystals of the compounds **1** and **3** were mounted in a nylon cryoloop for X-ray data collection. The diffraction data were collected at 100 K (**1**) and 173 K (**3**) on a Rigaku R-AXIS Rapid imaging-plate-mounted two-dimensional X-ray diffractometer with graphite-monochromated Cu-Kα radiation (λ = 0.154186 nm), using an ω-scan technique. Numerical absorption correction was applied by using fully automatic data collection software Rapid AUTO. The structure was solved by the direct method using SHELXS 2013[54], and all non-hydrogen atoms were refined anisotropically with full-matrix least square technique based on F^2 value. Hydrogen atoms were added geometrically.

On the other hand, compounds **2** and **4** were obtained as polycrystalline solids. Then, powder X-ray crystal structure analyses were performed. For precise structural analysis, high resolution powder X-ray diffraction data were collected at 300 K on a transmission geometry diffractometer with a Debye–Scherrer camera having an imaging plate (IP) at the BL02B2 of SPring-8 (λ = 0.99752(2) Å) (Hyogo, Japan) using the powder samples loaded in 0.3 mm glass capillaries. The unit cells were found in NTREOR[55] and refined in the Le Bail method[56] using EXPO2009 software[57]. For compound **2**, the initial structural model was obtained in the direct method in EXPO2009 and the missing parts were modelled by using Accelrys Materials Studio software. The model was refined with soft geometrical restraints excluding a few diffraction peaks from tiny amount of an impurity phase and the analysis reached convergence in the Rietveld method using Rietan-FP.[58] (Supporting information, Figure 2S) The final model of compound **2** is in the space group *Cmca* (no. 64), a = 28.4774(5), b = 9.4694(1), c = 18.8921(3) Å, V = 5094.5(1) Å^3, and Z = 8. Compound **4** was indexed in orthorhombic space group *Pbam* with unit cell parameters of a = 20.377(2), b = 8.0272(2), c = 17.873(1) Å, V = 2923.7(3) Å^3, and Z = 4. The space group is exactly the same as that of a MOF reported by Clearfield *et al*, and both the unit cell parameters are similar to each other (*Pbam* (no. 55), a = 20.3854(16), b = 7.9172(6), c = 17.7768(14) Å, V = 2869.1(4) Å^3, and Z = 4).[47] The differences of each unit cell parameter are less than 2 % despite the different measurement temperatures (room temperature for compound **4** and 110 K for the MOF reported by Clearfield *et al*.); for parameter a, b, c, and V, the differences are 0.05 %, 1.39 %, 0.54 %, and 1.90 %, respectively. The framework of the MOF reported by Clearfield *et al*. is composed of copper(II) ion, H_2bpt^{4-} ion, water, and bpp molecules, which are contained in the starting mixture of **4**. So, we concluded that compound **4** was an essentially identical material to the reported one, which was obtained through a solvothermal synthesis in DMF with a different metal source and a different mixing ratio. The results of the following FT-IR, TG, and elemental analysis are consistent with the conclusion in spite of different guest solvent. The discussion concerning compound **4** below is, therefore, based on the reported crystal structure. Details of crystallographic parameters of the compounds **1**-**3** are summarized in Table 1.

Table 1. Crystal structure data of compounds **1** - **3**.

	1	2	3
Formula	$C_{16}H_{10}Cu_2N_2O_{18}P_6$	$C_{16}H_{25}Cu_2N_2O_{15}P_3$	$C_{18}H_{19}Cu_2N_2O_{15}P_3$
M_w	831.16	705.39	723.21
T [K]	100	300	173
λ [Å]	1.54187	0.99752	1.54187
Crystal dimensions [mm]	0.30 × 0.30 × 0.05	-	0.25 × 0.20 × 0.15
Crystal system	Monoclinic	Orthorhombic	Orthorhombic
Space group	$P2_1/c$	*Cmca*	*Cmca*
a [Å]	9.08250(10)	28.4774(5)	33.7186(11)
b [Å]	18.5934(3)	9.4694(1)	7.9481(3)
c [Å]	7.86290(19)	18.8921(3)	20.5910(5)
β [°]	109.3520(19)	90	90
V [Å^3]	1252.82(3)	5094.5(1)	5518.4(3)
Z	4	8	8
$D_{calcd.}$ [g mol^{-1}]	2.203	1.894	1.741
F(000)	824	2864	2911
$R1$[a] or R_B[b]	0.0323	0.0318 (R_B)	0.0464
$wR2$[c] or R_{wp}[d]	0.0916	0.01706 (R_{wp})	0.1164

[a] $R1 = \Sigma||F_o| - |F_c||/\Sigma|F_o|$. [b] $R_B = \Sigma|I_o - I_c||/\Sigma|I_o|$. [c] $wR_2 = \{\Sigma\{(F_o^2 - F_c^2)^2/\Sigma[w(F^2_o)^2]\}^{1/2}$. [d]] $R_{wp} = \{\Sigma\{w(y_o - y_c)^2/\Sigma[w(y^2_o)^2]\}^{1/2}$.

Results and Discussion

Crystal structures of compounds 1-4

The crystal structure of compound **4** was previously reported by Clearfield *et al*.[47] Compound **4** crystalizes in orthorhombic space group *Pbam*, and the asymmetric unit of the crystal structure contains one copper ion, half of a H_2bpt^{4-} ligand, and half of bpp ligand. Copper ion is in a five-coordination geometry and surrounded by three H_2bpt^{4-} ligands, one bpp ligand, and one water molecule. Compound **4** has layer motifs represented as $[Cu_2(H_2btp)(H_2O)_2]$ and the layers are pillared with bpp ligands to form quasi-rectangular pore windows of 10.3 × 14.0 Å estimated from the distances between copper ions. The pores are separated each other by the bpp molecules and the 2D layers, resulting in the formation of 1D channels along *b* axis. The estimated total accessible pore space is 791.9 $Å^3$ which is 27.6 % of the unit cell volume calculated by PLATON software.[59]

Both compounds **2** and **3** are crystallized in orthorhombic space group *Cmca*, which is a supergroup of the space group *Pbam* of compound **4**. The framework structures of compounds **2** and **3** are topologically identical to that of compound **4**. All copper (II) ions in compounds **2** and **3** are crystallographically equivalent and are in five-coordination geometry similar to the copper(II) ions in compound **4**. The copper (II) ions in compounds **2** and **3** are coordinated by one nitrogen atom from the N-donor ligands, and four oxygen atoms from three different phosphonates and from a water molecule that terminate framework connectivity. Each H_2bpt^{4-} ion bonds to six copper(II) ions through three phosphonate groups (Figure 2). In detail, one phosphonate group has four P-O-Cu bonds with four copper(II) ions and the other two have one P-O-Cu bond, respectively, in one H_2bpt^{4-} ion. The former phosphonate group should be doubly deprotonated to have two negative charges, and the latter two phosphonate groups should have one negative charge to keep the charge balance. The single crystal structure analysis of compound **3** supports the deprotonation of the phosphonate groups, because of the averaged shorter P-O bond (1.53 Å) in the former phosphonate groups and longer one (1.55 Å) in the latter phosphonate groups. As a result, the chemical composition of the layer is shown as $[Cu_2(H_2btp)(H_2O)_2]$. There are metal phosphonate clusters composed of four copper(II) ions and six phosphonate groups (Figure 3a), and these clusters are bridged by aromatic rings of H_2bpt^{4-} to form a distorted rhombic shaped network (Figure 3b). The network expands in *b*-*c* plane to form a 2D layer structure (Figure 3c and d). The 2D sheets are pillared with N-donor ligands through copper(II) ions with different interlayer distances of 14.2 Å (**2**) and 16.9 Å (**3**) to construct 3D open framework structures, in which the N-donor ligands are aligned parallel to each other along *b* axis with the distance of 3.4-3.5 Å (**2**) and 3.2-3.6 Å (**3**) (Figure 3e and 4). As one can see in the figure 3e and 4, both the compounds has preudo-rectangular

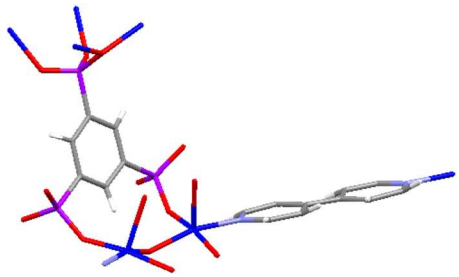

Figure 2. View of the asymmetric unit of compound **2**. All solvents have been omitted for clarity. (cyan, copper; gray, carbon; right blue, nitrogen; red, oxygen; purple, phosphorus; white, hydrogen)

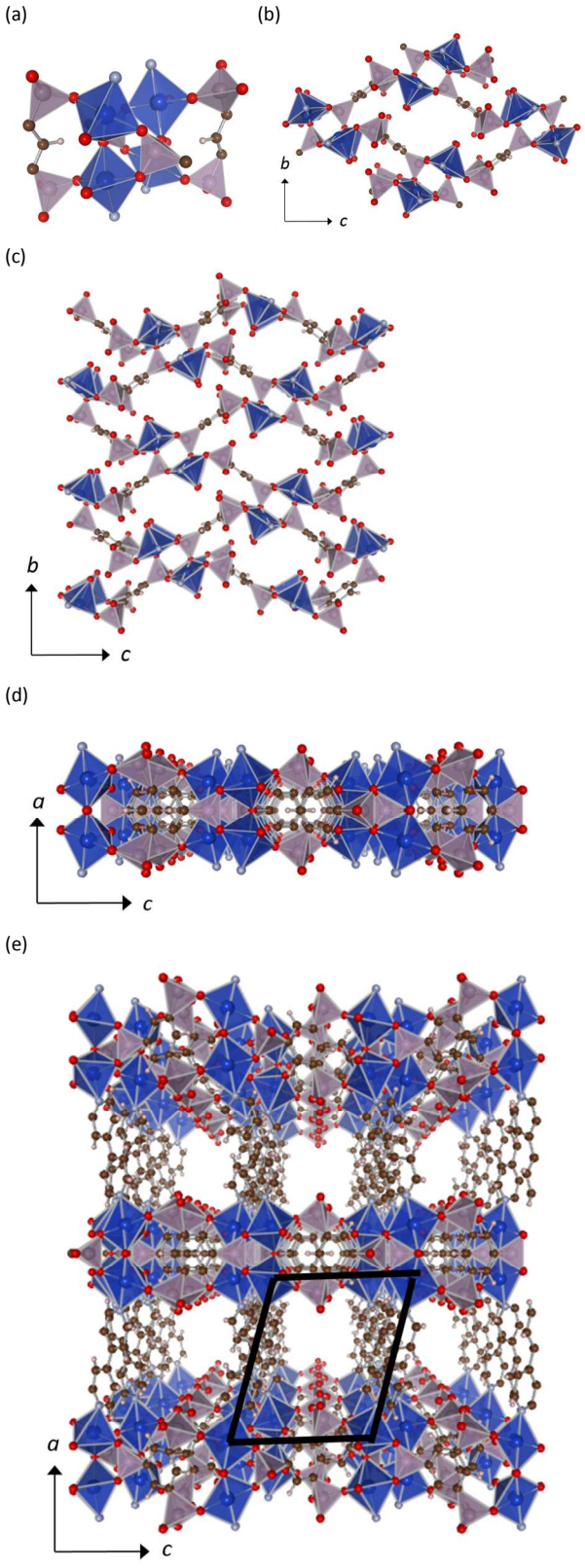

Figure 3. (a) Metal phosphonate cluster, (b) rhombic network along *a* axis, layer structure (c) along *a* axis and (d) along *b* axis, and (e) 3D pillared layered framework structure of compound **2**.

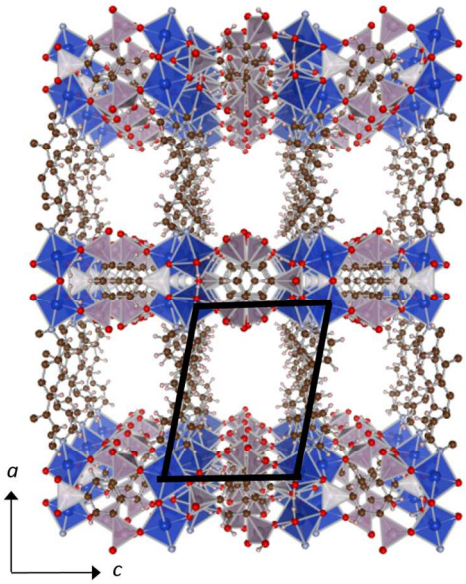

Figure 4. 3D pillared layered framework structure of compound **3**.

shaped pores along the *b* axis.

As mentioned above, the crystal structures of compounds **2**-**4** are topologically identical and are recognized as isostructural pillared layered materials with different interlayer distances of 14.2 Å (**2**), 16.9 Å (**3**), and 17.8 Å (**4**). The layer structures in compounds **2**, **3**, and **4** are closely resemble but slightly different with each other. In compounds **2**-**4**, the network topology in the layers is exactly the same, and however, the orientation of the clusters is different due to the different orientation of the phosphonate groups. The difference of the layer structures appears in the occupied area of the layers. The calculated area per $[Cu_8(H_2btp)_4]$ unit, which correspond to the unit cell area in *b*-*c* plane for compounds **2** and **3**, and in *a*-*b* plane for compound **4**, are 179 $Å^2$ (**2**), 164 $Å^2$ (**3**), and 161.3 $Å^2$ (**4**), respectively, indicating that the layer structures of compounds **3** and **4** are more similar to each other and more dense than the layer in compound **2**. Compound **3** and **4** also have pseudo-rectangular shaped 1D pores. Using the atomic centers of copper(II) ions as points of the rectangular, we measured the edge of the rectangular as *ca*. 9.8 × 11.2 Å (**2**), 10.4 × 13.4 Å (**3**), and 10.3 × 14.0 Å (**4**). The accessible void is 1217 $Å^3$ (23.9 %) for compound **2**, 1280.2 $Å^3$ (23.2 %) for compound **3**, and 791.9$Å^3$ (27.6 %) for compound **4**, respectively, calculated by PLATON software.[59] Because of the half value of Z (Z = 4) in compound **4** compared with that in compounds **2** and **3** (Z = 8), the void in compound **4** is doubled to be 1583.8 $Å^3$ for easy comparison. As a results, it is clear that the void volume is increased by using longer N-donor ligands.

Single crystal X-ray analysis revealed that compound **1**, $[Cu_2(H_4btp)_2(pyr)]$, crystallizes to form a dense structure in the

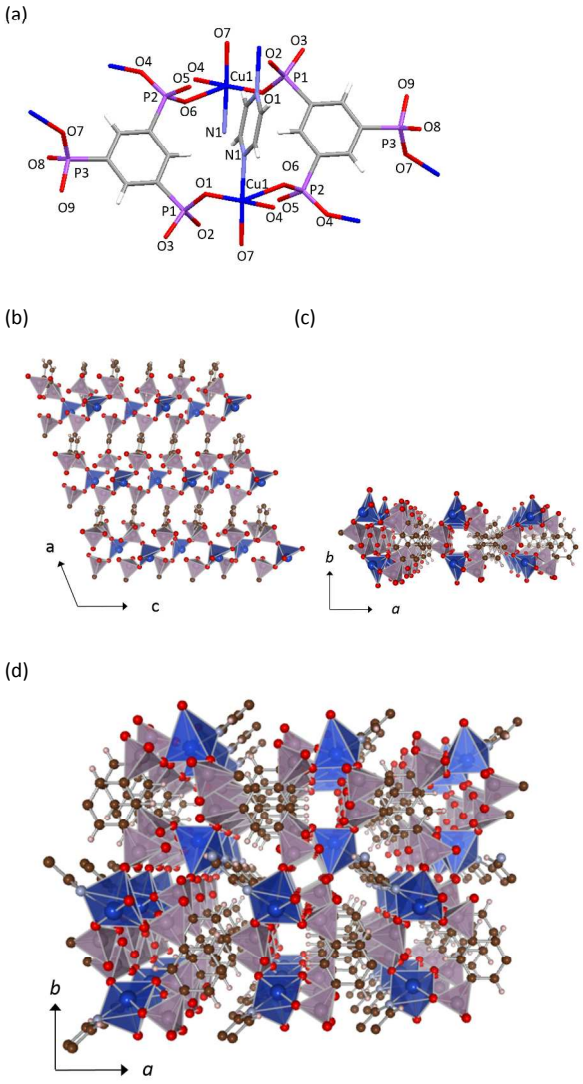

Figure 5. (a) The local coordination environment in the compound **1**. Symmetry code: x, y, z; -x, ½+y, ½+z; -x, -y, -z; x, ½-y, ½+z. Layer structures (b) along *b* axis and (c) along *c* axis, and (d) the 3D framework structure of the compound **1**.

space group $P2_1/c$, which is essentially a different structure from compounds **2**-**4**. All copper(II) ions in compound **1** are crystallographically equivalent and the local coordination geometry around the copper(II) ions is described as a distorted square-pyramidal (Figure 5a). The copper(II) ions are coordinated by one nitrogen atom and four oxygen atoms, which is the same first coordination environment as those of the compound **2**-**4**. Each copper(II) ion is coordinated by four different phosphonate groups through oxygen atoms and one pyr ligand through a nitrogen atom. Among the bonds, one bond between Cu(1) and O(6) is much longer than the other bonds (Table 2). The H_4bpt^{2-} ligands are parallel-aligned along the *c* axis with the average distance of 4.1 Å and bridged by copper(II) ions in the direction of *a* axis to form 2D copper phosphonate sheets (figure 5b and c). The 2D sheets are pillared with pyr ligands and furthermore bridged through the

Table 2. Selected bond length [Å] and angles [°] in compound **1**.

Cu1 – O1	1.920(2)	O1 - Cu1 – O7	90.66(8)
Cu1 – O4	1.938(2)	O1 – Cu1 – O4	167.57(9)
Cu1 – N1	2.041(2)	O1 – Cu1 – N1	88.74(9)
Cu1 – O7	1.937(2)	O7– Cu1– O4	92.07(8)
Cu1 – O6	2.525(2)	O7 – Cu1 – N1	175.57(9)
		O4– Cu1 – N1	89.44(9)

The values in parenthis mean estimated standard deviations.

long Cu(1)-O(6) bonds to form a 3D framework structure with interlayer distance of 9.3 Å. Because of the short interlayer distance and well developed bridging networks between the layers, compound **1** proves to have no accessible void space, which is estimated by PLATON software[59] using the single crystal structural data of compound **1**.

Thermal and structural investigation

TGA curves of compounds **1**-**4** are shown in Figure 3S (supporting information). All compounds show weight losses between room temperature to 200 ºC, which correspond to removal of water molecules inside and/or outside of the crystals. The weight loss percentages of compounds **2**-**4** are much higher than that of compound **1**, indicating larger amount of adsorbed water in the 1D pores. In compound **1**, the weight loss of 9.3 wt% between 200 - 400 ºC corresponds to the combustion of pyrazine ligand (calcd. 9.5 wt%). There is some large weight losses at higher temperature of 400 – 800 ºC, which should be owing to decomposition of H_4bpt^{2-} and condensation of hydroxyl groups of phosphonate groups. The expected final products at 1000 ºC are $Cu_2P_2O_7$ and P_2O_5, which correspond to 53.7 wt% of compound **1** (calcd. 53.3 wt%). The crystalline phase of $Cu_2P_2O_7$ was confirmed by XRD pattern of the residue after the TG measurement of compounds **1**, **3**, and **4**. In compound **2**, there are three-step weight losses of 30.2 wt% between 200 – 800 ºC, which should be due to removal of bpy ligands, decomposition of H_2bpt^{4-}, and condensation of hydroxyl groups of phosphonates (calcd. 29.9 wt%). The residue at 800 ºC was 52.8 wt% and estimated as $Cu_2P_2O_7$ and partially remaining P_2O_5 (calcd. 54.3 wt%). Compound **3** shows the weight loss of 3.0 wt% between 200 – 400 ºC, which should stem from condensation of the hydroxyl groups of H_2bpt^{4-} ligand (calculated at 2.5 %). The weight loss of 32.1 wt% of compound **3** in 400 – 800 ºC corresponds to decomposition of bpe and H_2bpt^{4-} ligand (calculated at 34.4 %). The TG curve of compound **4** is very similar to that of compound **3** and similar decomposition process should occur in the heating process. The weight percentage of the residue of compound **4** at 800 ºC is 60.2 wt%, which is well matched with the calculated percentage of $Cu_2P_2O_7$ and $0.9P_2O_5$ (60.3 wt%).

In order to investigate the structural stability of the framework, pillared layered compounds **2**-**4** were examined.

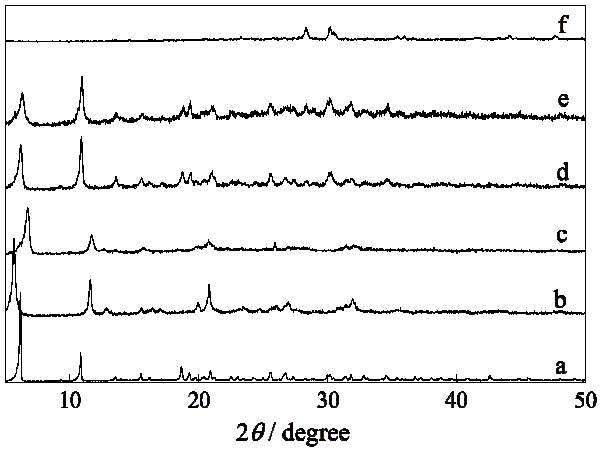

Figure 6. XRD patterns of the compound **2** in different conditions. (a) Pristine sample, (b) the sample heated at 100 ºC under vacuum, (c) the sample heated at 250 ºC under vacuum, (d) the sample b after water drop treatment, (e) the sample c after water drop treatment, and (f) the sample heated at 380 ºC.

TG analysis indicates that compound **2** releases water molecules at *ca*. 100 ºC and a part of bpy ligands at *ca*. 250 ºC with the help of a NMR experiment. Accordingly compound **2** was heated at 100 ºC and 250 ºC under vacuum, and the XRD patterns of the samples were measured after exposure to air (Figure 6). Through the removal of adsorbed water molecules, compound **2** kept the crystallinity with slight structural changes (Figure 6a to 6b). The partial removal of bpy ligands resulted in a different crystalline phase. Because of the broadening of diffraction peaks in the XRD patterns of the samples treated at 250 ºC, the vacuum-heating treatment should also induce decrease of crystallite size and/or crystal distortion (Figure 6a to 6c). Water was again dropped on the treated samples, resulting in recovery of XRD patterns similar to that of the pristine sample. These results suggest that compound **2** keeps the pillared layered network and shows structural reversibility during water accommodation/removal. It is interesting that the samples heated at 100 ºC and 250 ºC and with following water treatment show very similar XRD patterns, although the sample treated at 250 ºC has less amount of pillaring bpy molecules. Further heat treatment at 380 ºC gave almost amorphous and weak diffraction peaks recognized as $Cu_2P_2O_7$ phase, indicating collapse of the pillared layered structure. Compounds **3** and **4** release water molecules below 150 ºC and also showed similar structural change through accommodation/removal of guest water molecules (Supporting information, Figure 4S). Therefore, it should be noted that these pillared layered compounds have potential to show flexible nature through molecular accommodation depending on molecular species.

Gas adsorption analysis

Nitrogen adsorption isotherms were measured on compounds **2**-**4** at 77 K. Although all compounds **2**-**4** have accessible void space with pore entrances large enough to adsorb N_2 molecules (minimum dimension; 3.0 Å)[60] based on the crystal structures,

all compounds showed almost no uptake at low relative pressure. The BET surface area[61] of compounds are 1.1 m^2/g (**2**), 2.8 m^2/g (**3**), and 3.0 m^2/g (**4**), respectively. These results indicate that these compounds change their structures from open forms to non-porous forms through the removal of guest molecules by the pretreatment.

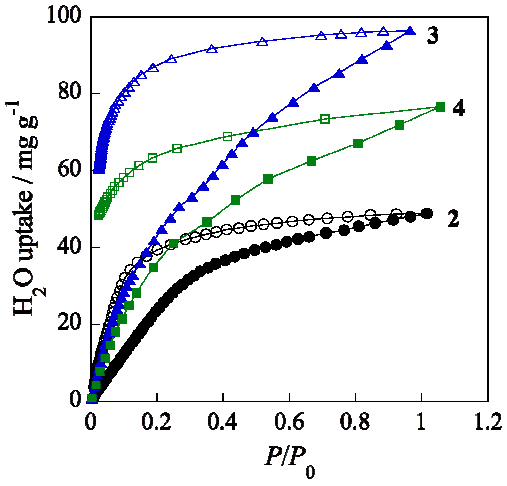

Figure 7. Adsorption isotherms of water vapor on the compound **2**-**4** at 303 K. Circle (**2**), triangle (**3**), and square (**4**). Filled and open symbols represent adsorption and desorption branches, respectively.

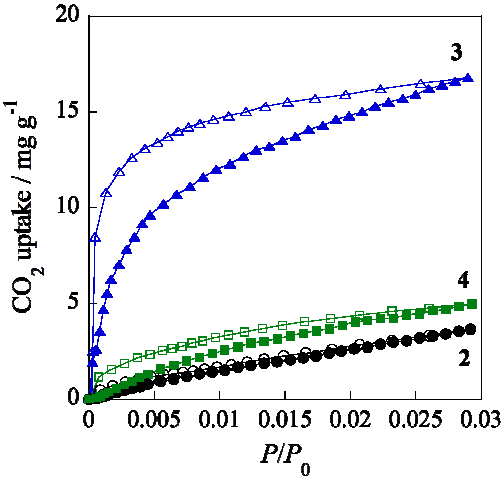

Figure 8. Adsorption isotherms of CO_2 on the compound **2**-**4** at 273 K. Circle (**2**), triangle (**3**), and square (**4**). Filled and open symbols represent adsorption and desorption branches, respectively.

As suggested by the results of TG, compounds **2**-**4** accommodate guest water molecules in the as-synthesized states and, the reversible structural changes of these compounds were observed by the XRD experiments with water drop treatment mentioned above. Therefore, compounds **2**-**4** potentially adsorb water vapor at ambient temperature. Figure 7 shows water vapor adsorption isotherms at 303 K on compounds **2**-**4**. As expected, all compounds show apparent adsorption uptakes at low relative pressure and large hysteresis loops, which are often observed in the adsorption isotherms of the flexible MOFs.[62–65] The pore volumes calculated by Dubinin-Radushkevich (DR) analysis[66] are 0.047 mL/g (**2**), 0.095 mL/g (**3**), and 0.083 mL/g (**4**), respectively. Compared with the void volumes estimated from the crystal structures, the pore filling percentages are 32 % (**2**), 61 % (**3**), and 46 % (**4**), respectively. It is not straightforward that the use of longer pillar ligands does not give higher adsorption uptakes. It should be noted that the percentages are in a considerably wide range and far from a complete filling of 100 %. These adsorption results suggest that compounds shows different adsorptivities of small molecules with different structural responses based on the molecular species and accommodation conditions.

Further investigation of molecular adsorptivities on compounds **2**-**4** were performed through CO_2 and ethanol adsorption experiments. Figure 8 shows CO_2 adsorption isotherms on compounds **2**-**4** at 273 K. Interestingly, compounds **2** and **4** has almost no uptake, and however, compound **3** shows a steep uptake at low pressure region like the water adsorption isotherm. By optimizing the degassing condition under vacuum at room temperature, compound **3** shows increase of CO_2 uptake up to 76 mg/g, indicating that compound **3** can essentially adsorb CO_2 molecules. In addition, all compounds **2**-**4** also adsorb ethanol vapor at 303 K below at P/P_0 = 1 with hysteresis loops in all isotherms (Supporting information, Figure 5S and 6S). These adsorption results with different kind of molecular species clearly indicate that these compounds show molecule-dependent gas adsorptivities. Because the molecular size of ethanol is larger than those of N_2 and CO_2, the adsorption properties of compounds **2**-**4** are not explained by a common molecular sieving effect.[60] As indicated by the XRD experiments with the water drop treatments, compounds **2**-**4** have framework flexibility, and after the pretreatment they should be nonporous forms as suggested by the N_2 adsorption experiments. These adsorption selectivities should appear as a result of the molecular affinities to the surfaces, inducing structural transformation in their flexible frameworks.[67–70]

Conclusions

In this paper, the synthesis, crystal structure, and gas adsorption properties of a series of copper phosphonates with different N-donor ligands were reported. As pillar molecules, four N-donor ligands of pyrazine (pyr), 4,4′-bipyridine (bpy), trans-1,2-bis(4-pyridyl)ethylene (bpe), and 1,3-bis(4-pyridyl)propane (bpp) were used. Compound **1**, $[Cu_2(H_4btp)_2(pyr)]$ (pyr = pyrazine), is a dense nonporous 3D framework compound composed of 2D layers bridged through the N-donor ligands pyrazine and phosphonate groups. Compounds **2**-**4** are topologically identical pillared layered materials, in which the 2D layers are expressed as $[Cu_2(H_2btp)(H_2O)_2]$ and different from that in compound **1**. The layers are pillared by N-donor ligands giving 3D open framework structures with quasi-rectangular shaped pores.

According to the crystal structures, both the pore size and the pore volume of compounds become larger with longer N-donor ligands. Compounds **2-4** show the reversible structural transformation accompanied with inclusion/removal of guest water molecules. Compounds **2-4** do not show N_2 adsorption at 77 K, while adsorb water vapor at 303 K. It should be noted that compounds **2-4** also adsorb ethanol which is larger in molecular size than that of N_2 and water. In addition, compound **3** adsorbs CO_2 molecules at 273 K. The selective adsorption properties of these compounds should be based not on molecular size but on the molecular affinities to the surfaces.

Acknowledgements

This work was partly supported by JSPS KAKENHI Grant No. 24550230. The synchrotron radiation experiemnts were performed at SPring-8 with the approval of the Japan Synchrotron Radiation Research Institute (JASRI) (Proposal No. 2010B1463).

Notes and references

Department of Applied Chemistry, Graduate School of Engineering, Tokyo University of Agriculture and Technology, 2-24-16 Naka-cho, Koganei, Tokyo 184-8588, JAPAN. E-mail: k-maeda@cc.tuat.ac.jp

† Electronic Supplementary Information (ESI) available: SEM image, TG curves, XRD patterns, CO_2 adsorption isotherm, and ethanol adsorption isotherms. CCDC 1053214-1053216. For ESI and crystallographic data in CIF see DOI: 10.1039/b000000x

1 S. R. Batten and R. Robson, *Angewandte Chemie International Edition*, 1998, **37**, 1460–1494.
2 P. J. Hagrman, D. Hagrman and J. Zubieta, *Angewandte Chemie - International Edition*, 1999, **38**, 2638–2684.
3 B. Moulton and M. J. Zaworotko, *Chemical Reviews*, 2001, **101**, 1629–1658.
4 O. M. Yaghi, O. K. M, N. W. Ockwig, H. K. Chae, M. Eddaoudi and J. Kim, *Nature*, 2003, **423**, 705–714.
5 D. Bradshaw, S. El-Hankari and L. Lupica-Spagnolo, *Chemical Society reviews*, 2014, **43**, 5431–43.
6 L. Carlucci, G. Ciani and D. M. Proserpio, *Coordination Chemistry Reviews*, 2003, **246**, 247–289.
7 G. Férey, *Chemical Society reviews*, 2008, **37**, 191–214.
8 W. Lu, Z. Wei, Z.-Y. Gu, T.-F. Liu, J. Park, J. Park, J. Tian, M. Zhang, Q. Zhang, T. Gentle Iii, M. Bosch and H.-C. Zhou, *Chemical Society Reviews*, 2014, **43**, 5561.
9 T. Zhang and W. Lin, *Chemical Society reviews*, 2014, **43**, 5982–5993.
10 V. Stavila, a. a. Talin and M. D. Allendorf, *Chem. Soc. Rev.*, 2014, **43**, 5994–6010.
11 K. Maeda, Y. Kiyozumi and F. Mizukami, *The Journal of Physical Chemistry B*, 1997, **101**, 4402–4412.
12 K. Maeda, *Microporous and Mesoporous Materials*, 2004, **73**, 47–55.
13 S. R. Miller, G. M. Pearce, P. a. Wright, F. Bonino, S. Chavan, S. Bordiga, I. Margiolaki, N. Guillou, G. Férey, S. Bourrelly and P. L. Llewellyn, *Journal of the American Chemical Society*, 2008, **130**, 15967–15981.
14 K. J. Gagnon, H. P. Perry and A. Clearfield, *Chemical Reviews*, 2012, **112**, 1034–1054.
15 M. Taddei, F. Costantino, A. Ienco, A. Comotti, P. V Dau and S. M. Cohen, *Chemical communications (Cambridge, England)*, 2013, **49**, 1315–7.
16 S. B. Acids, Z. Wang, J. M. Heising and A. Clearfield, 2003, 10375–10383.
17 H. L. Ngo, A. Hu and W. Lin, *Journal of Molecular Catalysis A: Chemical*, 2004, **215**, 177–186.
18 L. Ma, C. Abney and W. Lin, *Chemical Society Reviews*, 2009, **38**, 1248–1256.
19 S. Chessa, N. J. Clayden, M. Bochmann and J. a Wright, *Chemical communications (Cambridge, England)*, 2009, 797–799.
20 B. Zhang, D. M. Poojary, A. Clearfield and G. Peng, *Chemistry of Materials*, 1996, **8**, 1333–1340.
21 S. S. Bao, G. S. Chen, Y. Wang, Y. Z. Li, L. M. Zheng and Q. H. Luo, *Inorganic Chemistry*, 2006, **45**, 1124–1129.
22 M. Plabst, L. B. McCusker and T. Bein, *Journal of the American Chemical Society*, 2009, **131**, 18112–18118.
23 S. Maheswaran, G. Chastanet, S. J. Teat, T. Mallah, R. Sessoli, W. Wernsdorfer and R. E. P. Winpenny, *Angewandte Chemie - International Edition*, 2005, **44**, 5044–5048.
24 D. Cave, F. C. Coomer, E. Molinos, H. H. Klauss and P. T. Wood, *Angewandte Chemie - International Edition*, 2006, **45**, 803–806.
25 H.-C. Yao, J.-J. Wang, Y.-S. Ma, O. Waldmann, W.-X. Du, Y. Song, Y.-Z. Li, L.-M. Zheng, S. Decurtins and X.-Q. Xin, *Chemical communications (Cambridge, England)*, 2006, **1**, 1745–1747.
26 S. S. Bao, M. Li-Fang, Y. Wang, L. Fang, C. J. Zhu, Y. Z. Li and L. M. Zheng, *Chemistry - A European Journal*, 2007, **13**, 2333–2343.
27 Y. Z. Zheng, M. Evangelisti, F. Tuna and R. E. P. Winpenny, *Journal of the American Chemical Society*, 2012, **134**, 1057–1065.
28 T. Zheng, S.-S. Bao, M. Ren and L.-M. Zheng, *Dalton transactions (Cambridge, England : 2003)*, 2013, 16396.
29 G. Alberti and M. Casciola, *Solid State Ionics*, 2001, **145**, 3–16.
30 J. M. Taylor, R. K. Mah, I. L. Moudrakovski and C. I. Ratcliffe, *Journal of the American Chemical Society*, 2010, **132**, 14055–14057.
31 P. Ramaswamy, N. E. Wong and G. K. H. Shimizu, *Chemical Society reviews*, 2014, **43**, 5913–5932.
32 S. S. Bao, K. Otsubo, J. M. Taylor, Z. Jiang, L. M. Zheng and H. Kitagawa, *Journal of the American Chemical Society*, 2014, **136**, 9292–9295.
33 M. Bazaga-García, R. M. P. Colodrero, M. Papadaki, P. Garczarek, J. Zoń, P. Olivera-Pastor, E. R. Losilla, L. León-Reina, M. a G. Aranda, D. Choquesillo-Lazarte, K. D. Demadis and A. Cabeza, *Journal of the American Chemical Society*, 2014, **136**, 5731–5739.
34 G. Alberti, U. Costantino, S. Allulli and N. Tomassini, *Journal of Inorganic and Nuclear Chemistry*, 1978, **40**, 1113–1117.
35 G. Cao, H. Lee, V. M. Lynch and T. E. Mallouk, *Inorg. Chem.*, 1988, **27**, 2781–2785.
36 Y. Zhang and A. Clearfield, *Inorganic chemistry*, 1992, **31**, 2821–2826.
37 G. Alberti, M. Casciola, U. Costantino and R. Vivani, *Adv. Mater.*, 1996, **8**, 291–303.
38 K. Maeda, Y. Hashiguchi, Y. Kiyozumi and F. Mizukami, *Bulletin of the Chemical Society of Japan*, 1997, **70**, 345–349.
39 M. B. Dines, P. M. Digiacomo, K. P. Callahan, P. C. Griffith, R. H. Lane and R. E. Cooksey, *ACS Symp. Ser.*, 1982, **13**, 223–240.

40 D. M. Poojary, L. a Vermeulen, E. Vicenzi, A. Clearfield and M. E. Thompson, *Chem. Mater.*, 1994, **6**, 1845–1849.
41 D. K. Cao, S. Gao and L. M. Zheng, *Journal of Solid State Chemistry*, 2004, **177**, 2311–2315.
42 C. A. Merrill and A. K. Cheetham, *Inorganic chemistry*, 2007, **46**, 278–284.
43 K. D. Demadis, A. Panera, Z. Anagnostou, D. Varouhas, A. M. Kirillov and I. Císařová, *Crystal Growth and Design*, 2013, **13**, 4480–4489.
44 D. Kong and A. Clearfield, *Cryst. Growth Des.*, 2005, **5**, 1767–1773.
45 J. L. Song and J. G. Mao, *Journal of Solid State Chemistry*, 2005, **178**, 3514–3521.
46 S. M. Ying and J. G. Mao, *Crystal Growth and Design*, 2006, **6**, 964–968.
47 D. Kong, J. Zon, J. Mcbee and A. Clearfield, *Inorganic chemistry*, 2006, **45**, 977–986.
48 J. M. Taylor, A. H. Mahmoudkhani and G. K. H. Shimizu, *Angewandte Chemie - International Edition*, 2007, **46**, 795–798.
49 K. Maeda, H. Hatasawa, K. Kawawa, N. Nagayoshi and Y. Matsushima, *Chemistry Letters*, 2011, **40**, 215–217.
50 K. Maeda, R. Takamatsu, M. Mochizuki, K. Kawawa and A. Kondo, *Dalton transactions (Cambridge, England : 2003)*, 2013, **42**, 10424–10432.
51 T. Araki, A. Kondo and K. Maeda, *Chemical Communications*, 2012, **49**.
52 T. Araki, A. Kondo and K. Maeda, *Chem. A. Eur. J.*
53 M. Henn, K. Jurkschat, D. Mansfeld, M. Mehring and M. Schürmann, *Journal of Molecular Structure*, 2004, **697**, 213–220.
54 G. M. Sheldrick, *Acta Crystallographica Section A: Foundations of Crystallography*, 2007, **64**, 112–122.
55 A. Altomare, C. Giacovazzo, A. Guagliardi, A. G. G. Moliterni, R. Rizzi and P. E. Werner, *Journal of Applied Crystallography*, 2000, **33**, 1180–1186.
56 A. Le Bail, H. Duroy and J. L. Fourquet, *Materials Research Bulletin*, 1988, **23**, 447–452.
57 A. Altomare, M. Camalli, C. Cuocci, C. Giacovazzo, A. Moliterni and R. Rizzi, *Journal of Applied Crystallography*, 2009, **42**, 1197–1202.
58 F. Izumi and K. Momma, in *Solid State Phenomena*, 2007, vol. 130, pp. 15–20.
59 P. van der Sluis and A. L. Spek, *Acta Crystallographica Section A*, 1990, **46**, 194–201.
60 D. W. Breck, *Zeolite molecular sieves: structure, chemistry, and use*, Wiley, 1973.
61 S. Brunauer, P. H. Emmett and E. Teller, *Journal of the American Chemical Society*, 1938, **60**, 309–319.
62 X. Zhao, B. Xiao, A. J. Fletcher, K. M. Thomas, D. Bradshaw and M. J. Rosseinsky, *Science (New York, N.Y.)*, 2004, **306**, 1012–1015.
63 A. Kondo, H. Noguchi, S. Ohnishi, H. Kajiro, A. Tohdoh, Y. Hattori, W. C. Xu, H. Tanaka, H. Kanoh and K. Kaneko, *Nano Letters*, 2006, **6**, 2581–2584.
64 R. Kotani, A. Kondo and K. Maeda, *Chemical Communications*, 2012, **48**, 11316–11318.
65 A. Kondo, H. Noguchi, L. Carlucci, D. M. Proserpio, G. Ciani, H. Kajiro, T. Ohba, H. Kanoh and K. Kaneko, *Journal of the American Chemical Society*, 2007, 12362–12363.
66 M. M. Dubinin, *Chemical Reviews*, 1960, **60**, 235–241.
67 R. Kitaura, K. Seki, G. Akiyama and S. Kitagawa, *Angewandte Chemie - International Edition*, 2003, **42**, 428–431.
68 A. Kondo, A. Chinen, H. Kajiro, T. Nakagawa, K. Kato, M. Takata, Y. Hattori, F. Okino, T. Ohba, K. Kaneko and H. Kanoh, *Chemistry - A European Journal*, 2009, **15**, 7549–7553.
69 A. Kondo, H. Kajiro, H. Noguchi, L. Carlucci, D. M. Proserpio, G. Ciani, K. Kato, M. Takata, H. Seki, M. Sakamoto, Y. Hattori, F. Okino, K. Maeda, T. Ohba, K. Kaneko and H. Kanoh, *Journal of the American Chemical Society*, 2011, **133**, 10512–10522.
70 A. Kondo, N. Kojima, H. Kajiro, H. Noguchi, Y. Hattori, F. Okino, K. Maeda, T. Ohba, K. Kaneko and H. Kanoh, *The Journal of Physical Chemistry C*, 2012, **116**, 4157–4162.

A graphical and textual abstract

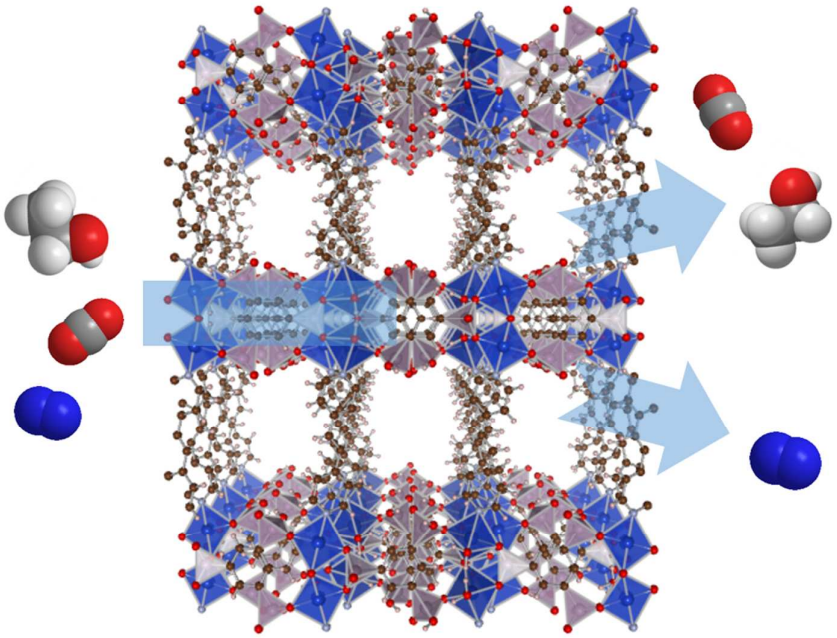

New layered copper phosphonates with N-donor pillaring ligands were synthesized and adsorption properties of them were investigated.